Materials International
Open Access Journal (ISSN: 2668-5728)

Article
Volume 7, Issue 2, 2025, 12
https://doi.org/10.33263/Materials72.012

Enhanced Filtration Performance of Nanocellulose and Chitosan-Based Nano Filters in Nickel Removal: Impact of Chemical Conditions

Kenechukwu Keluo Onyechi [1,*], Chinenye Adaobi Igwegbe [2,3,*]

[1] Department of Pharmaceutics and Pharmaceutical Technology, Nnamdi Azikiwe University, P. M. B. 5025, Awka 420218, Nigeria; chigoziri.njoku@futo.edu.ng;
[2] Department of Chemical Engineering, Nnamdi Azikiwe University, P.M.B. 5025, Awka 420218, Nigeria
[3] Department of Applied Bioeconomy, Wroclaw University of Environmental and Life Sciences, Poland
* Correspondence: ca.igwegbe@unizik.edu.ng/ chinenyeigwegbe@gmail.com/ chinenye.igwegbe@upwr.edu.pl (C.A.I.); kk.onyechi@unizik.edu.ng (K.K.O.);

Scopus Author ID 57202015214
Received: 28.06.2024; Accepted: 2.01.2025; Published: 13.02.2025

Abstract: This study investigates the filtration efficiency and morphological characteristics of nanocellulose, chitosan, and composite filters. It explores the impact of varying chemical conditions (molarities and pH levels) on filtration rate, velocity, viscosity, and pressure difference. Three types of filters were produced: pure chitosan (Batch A), pure nanocellulose (Batch B), and a nanocellulose-chitosan composite (Batch C). Characterization involved particle size analysis, zeta potential measurement, SEM imaging, and filtration performance tests under varied pH and molarity conditions. Nanocellulose exhibited superior mechanical properties, with a tensile strength of 82.8 MPa, surpassing chitosan (39.2 MPa) and the composite (124.6 MPa). Quantitative results indicated that Batch B (nanocellulose) filters had the lowest pressure drops ($2.14x10^{-11}$ and $2.21x10^{-11}$ Pa) in basic conditions (0.1M and 0.5M NaOH), showing reduced resistance and improved efficiency in alkaline environments. Batch B also exhibited the highest filtration velocities across various pH levels, maintaining a rate of 7.96×10^{-5} m/s even under acidic conditions (0.1M and 0.5M HCl), outperforming chitosan and composite filters. Filtration tests demonstrated nanocellulose filters achieving purity levels of 99.99% across pH ranges. The statistical analysis revealed no significant difference in the performance of chitosan, nanocellulose, and nanocellulose-chitosan filter papers (P-value = 0.986). At the same time, the pH conditions significantly affected nickel removal efficiency, with lower pH levels showing reduced performance (P-value < 0.05). This study underscores the potential of nanocellulose-based materials for advanced filtration applications, offering enhanced efficiency in diverse environmental conditions.

Keywords: nanocellulose; water remediation; heavy metal removal; nano filters; environmental sustainability.

1. Introduction

The most pressing challenge of the current era revolves around ensuring an adequate supply of clean and affordable water for all. This challenge is exacerbated by factors such as population growth, the impacts of climate change, and the declining quality of water sources [1]. Nanotechnology offers promising solutions to global challenges, especially in environmental remediation. Among these advancements, nanocellulose-based nano filters have

emerged as a sustainable and effective means for heavy metal removal from water sources [2-4]. Heavy metal contamination poses a significant threat to human health and ecosystem integrity, with deleterious effects ranging from acute toxicity to long-term environmental degradation [5-7]. Although widely employed, conventional remediation methods, including chemical precipitation, coagulation, and membrane filtration, often exhibit limitations in efficiency, cost-effectiveness, and sustainability [8,9]. Thus, there is a compelling imperative to develop alternative approaches that are effective, environmentally benign, and economically viable.

Nanocellulose has recently gained attention as a promising material for addressing the challenges posed by water contamination, especially nickel [10-12], which is a common and harmful heavy metal pollutant [13]. Nickel contamination is particularly problematic due to its toxicity even at low concentrations, its persistence in the environment, and its ability to bioaccumulate, posing significant health risks to humans and ecosystems [14]. Nanocellulose and chitosan represent two promising materials for addressing the challenges of heavy metal pollution in water. Nanocellulose, a nanomaterial derived from renewable biomass sources such as wood pulp or agricultural residues, has garnered considerable attention owing to its exceptional properties and versatile applications [15-17]. Unlike conventional cellulose materials, nanocellulose possesses a hierarchical structure with nanoscale dimensions, endowing it with unique mechanical, optical, and physicochemical attributes [16]. Of particular relevance to water remediation is nanocellulose's high surface area-to-volume ratio, abundant surface hydroxyl groups, and biocompatibility, which render it highly amenable to functionalization and tailored modification for targeted pollutant removal [18-20].

On the other hand, chitosan, derived from chitin, offers advantages, including biodegradability [21], antimicrobial properties [22], and the ability to form stable complexes with metal ions through chelation and electrostatic interactions [23,24]. Combining these two materials into composite filters can achieve synergistic benefits, such as enhanced mechanical stability, improved porosity, and increased adsorption capacity, optimizing their performance in diverse environmental conditions. The development of nanocellulose-chitosan composite filters also addresses a gap in the existing literature regarding the effective removal of specific heavy metals such as nickel. Developing and characterizing nanocellulose-chitosan composite filters are crucial to advancing sustainable filtration technologies. These filters exhibit superior performance in heavy metal removal and contribute to reducing environmental impact through their renewable and biodegradable nature [2,25]. Understanding these composite materials' structural morphology, surface chemistry, and filtration efficiency under different chemical conditions (such as varying pH levels and molarities) is essential for tailoring their application in real-world scenarios, from industrial wastewater treatment to portable water purification systems.

Moreover, this study addresses the critical need for comprehensive performance evaluation of nanocellulose and chitosan-based filters across various environmental conditions. By systematically analyzing parameters such as filtration rate, pressure drop, particle retention efficiency, and durability, we objectively assess their suitability for practical applications [26]. In addition to material characterization, this study introduces a rigorous statistical analysis to evaluate the performance differences among filter types and the impact of varying chemical conditions on nanofiltration efficiency. Employing descriptive statistics and analysis of variance (ANOVA), the analysis reveals how different pH environments influence removal efficiency, highlighting the effectiveness of specific conditions and identifying those

significantly impair performance. This approach fills a research gap by providing insights into the specific conditions that maximize or hinder filter performance in nickel removal. This statistical approach enhances the reliability of our findings, offering a nuanced understanding of the interaction between filter composition and environmental factors.

The findings presented herein advance fundamental understanding and pave the way for optimizing the design and fabrication of nano filters capable of meeting stringent environmental standards and operational requirements. Comprehensive characterization of filter properties—hydrodynamic diameter, porosity, permeability, surface area, and tensile strength—will provide critical insights into their performance under varying chemical conditions (pHs and molarities) for advanced filtration applications in different wastewaters, particularly focusing on nickel removal. This study delves into the forefront of nanotechnology-driven solutions for sustainable water remediation. By elucidating the intricate interplay between material properties, chemical conditions, and filtration performance, we aim to inspire future research endeavors to enhance filtration technologies' efficiency, affordability, and environmental compatibility. The insights gained from this study are poised to inform researchers striving to address the pressing challenges of global water quality management, environmental sustainability, and practical insights for improving water purification and industrial filtration systems, particularly on mitigating nickel pollution.

2. Materials and Methods

2.1. Collection of materials.

Semi-synthetic biopolymers (chitosan and nanocellulose) were bought from Onitsha Chemicals Market, Anambra State, Nigeria. While this study utilized semi-synthetic nanocellulose and chitosan to ensure consistency and control over the material properties, it is important to note that the fundamental components of these materials are derived from renewable resources. Nanocellulose can be extracted from agricultural waste such as crop residues and wood pulp, while chitosan is typically derived from chitin, found abundantly in crustacean shells. Semi-synthetic versions in this research are intended to standardize the experimental conditions and ensure the reproducibility of results.

2.2. Determination of particle sizes and zeta potential of chitosan and nanocellulose particles.

The nanoparticles' mean hydrodynamic diameter, polydispersity, and zeta potentials were determined using zeta sizer nano Zs equipped with a 633 nm laser source for particles suspended in deionized water. The analysis was performed at room temperature (26°C) at a scattering angle of 90° after the appropriate solution of 1ml dispersion of stock (1 wt %) in 10 mL of distilled water and filtered with double covalent 0.1 um filters. Each value reported is an average of multiple measurements.

2.3. Formulation of filter papers.

A sludge of 20 wt% natural and semi-synthetic (commercial) biopolymer was prepared according to Table 1 using 5 wt% acetic acid solution of adjusted pH 4.7. Polyacrylamide solution was prepared by dissolving 5 g in 95 g of 5 wt % acetic acid solution. The solution was stirred at 60 rpm (to prevent air bubble trapping) under 26°C for 2 hours and allowed to stand for 24 hours until a completely clear solution was achieved. A covalent cross-linker was

also prepared by incubating N-N-methyl bisacrylamide of 0.1 wt% in distilled water and stirred at 60 rpm under 26°C for 2 hours and allowed to stand for 24 hours. The cross-linker was added to the polyacrylamide solution in the ratio of 1:3 to create functional group linkage for binding the natural polymers. The natural polymer sludge was then suspended in the polyacrylamide solution and homogenized at 1200 rpm for 1 hour under 26°C. The pH was then adjusted to 7 using a 1N sodium hydroxide solution. The polymer mixtures were collected by centrifuging for 1 hour at 4000 rpm or allowed to stand for 48 hours. The mixtures were washed with distilled water to pH 7, centrifuged for another hour at 4000 rpm, cast on a stainless mold, and freeze-dried at 4°C to form filter papers.

Table 1. The formulation for the semi-synthetic/commercial bio-polymeric filter paper batches.

Polymers	Batch A (%)	Batch B (%)	Batch C (%)
Polyacrylamide hydrogel	30	30	30
Nanocellulose	-	70	35
Chitosan	70	-	35

2.4. Morphological characterization.

Scanning electron microscopy (SEM) was performed to examine the structural change of samples using SEM (Phenom ProX) by Phenom-World Eindhoven, Netherlands. For each formulation, a cut-out sample was placed on a double adhesive sample stub and coated with a sputter coater by Quorum Technologies model Q150R, with 5 nm of gold. Thereafter, it was taken to the chamber of the SEM machine, where it was viewed via NaVCaM for focusing and little adjustment. It was then transferred to SEM mode, was focused, and brightness contrasting was automatically adjusted. Afterward, the morphologies of different magnifications were stored in a USB stick.

2.5. Determination of filter paper properties.

The procedures for measuring critical parameters of the filter membranes and evaluating their performance under various conditions, including heavy metal and bacterial suspensions, are detailed in this section.

2.5.1. Thickness measurement of filter paper (membrane).

The thickness of the filter medium (L) was determined using a vernier caliper.

2.5.2. Determination of filter membrane area.

The area (m^2) of the filter membrane was calculated using the diameter of the membrane. The formula used is:

$$A = \pi r^2 \qquad (1)$$

Where r is the radius of the filter membrane (that is, diameter/2) and π is 3.142.

2.5.3. Porosity measurement of the filter membrane.

The porosity of the filter membrane was measured by immersing it in a known volume of deionized water (v1) for 5 minutes. The increased volume (v2) after immersion and the final volume (v3) after removing the membrane were noted. This was repeated thrice to calculate the average volume. Porosity (e) was calculated using the following equations [27,28]:

$$e = \frac{v1-v3}{v2-v3} \times 100 \qquad (2)$$

2.5.4. Permeability of the filter membrane.

The permeability of a porous filter medium describes how easily a fluid can flow through it [29]. The permeability of the filter membrane was determined using a Buchner funnel. Four filter mediums were wetted with deionized water, and 50 ml of deionized water was poured through them. The volume of the filtrate after 5 minutes was recorded. This process was repeated with different filter medium configurations - single (L1), double (L2), triple (L3) and quadruple (L4). A graph of $log\ v/t$ (Table S1, see supplementary) against $log\ 1/L$ was plotted (Figure S1 in supplementary file) to determine permeability (k) using Darcy's equation [30-32]:

$$v/t = \frac{kA\Delta P}{\eta L} \qquad (3)$$

Where the slope (x) is $\frac{kA}{\eta}$ so $k = \frac{\eta x}{A}$ and ΔP is assumed to be constant.

(Q is the volumetric flow rate (m³/s), k is the permeability of the medium (m²), A is the cross-sectional area (m²), ΔP is the pressure difference (Pa), η is the dynamic viscosity (Pa·s), and L is the length of the medium (m)).

2.5.5. Calculation of the specific surface area of the filter medium.

The specific surface area of the filter medium was calculated using the Kozeny-Carman (K–C) equation [31]:

$$v/t = \frac{A\Delta P e^3}{\eta S^2 CL(1-e)^2} \qquad (4)$$

The viscosity of the fluid flowing through the filter medium is denoted by η, while ΔP represents the pressure drop across the filter medium. The symbol e stands for the porosity of the filter medium, and S represents its specific surface area. L denotes the thickness or length of the filter medium. The constant C, which accounts for the pore space, is given as 5. This leads to Eqn. 5:

$$v/t = \frac{A\Delta P e^3}{5\eta S^2 L(1-e)^2} \qquad (5)$$

By substituting the variables from Darcy's and Poiseuille's equations, the specific surface area (S) was determined.

Substituting v/t for Darcy's equation (Eqn. 3) and Poiseullie's equation

(a) For Darcy's equation we have

$$k = \frac{e^3}{5S^2(1-e)^2} \qquad (6)$$

$$S = \sqrt{\frac{e^3}{5k(1-e)^2}} \qquad (7)$$

(b) Poiseullie's equation is given as Eq. 8 [33]

$$v/t = \frac{\pi r^4 \Delta P}{8\eta L} \qquad (8)$$

After substituting for v/t we have

$$r^2/8 = \frac{e^3}{5S^2(1-e)^2} \qquad (9)$$

$$S = \sqrt{\frac{8e^3}{5r^2(1-e)^2}} \qquad (10)$$

2.5.6. Determination of filtration rate, filtration velocity, viscosity, and pressure difference on varied molarities and pH of the nickel suspension.

The experiment aims to evaluate how nano filters perform under varying pH conditions of different effluents. This investigation is crucial for determining the optimal pH range that ensures consistent and effective filtration, addressing the specific requirements of diverse industrial and environmental applications. Nickel powder was suspended in different molarities of known pH levels (deionized H_2O with pH 6.8, 0.1M HCl (pH 0.4), 0.5M HCl (pH 1.2), 0.1M NaOH (pH 13), 0.5M NaOH (pH 14). Suspension 20 wt% was made, and the viscosity was determined using Brookfield Viscometer (Pa.s). The suspension was poured on the Buchner funnel (Fig. 1) containing the nano filters, and the time of collection (t) of different volumes of filtrate (5, 10, 15, 30, and 40 mL) was recorded (see Table S2 in supplementary file). The process was repeated thrice to calculate the average time. A graph of the volume of filtrate against time was plotted to determine the filtration rate (slope) (Figure S2a-e in supplementary file). The filtration rate (Q) and velocity (V) were calculated using [34]:

$$^{v}/_{t} = Q \quad (11)$$

$$Q = VA \quad (12)$$

$$V = {}^{Q}/_{A} \quad (13)$$

Where V is the velocity of filtrate across the filter membrane.

2.5.7. Calculation of pressure difference (ΔP).

The pressure drop across the filter is an important factor influencing the energy consumption and overall efficiency of the filtration process [35]. The pressure difference across the filter medium was determined using Darcy's and Poiseuille's equations:

(a) Darcy's equation

$$^{v}/_{t} = \frac{kA\Delta P}{\eta L}; V = \frac{k\Delta P}{\eta L} \quad (14)$$

$$\Delta P = \frac{Q\eta L}{kA} = \frac{V\eta L}{k} \quad (15)$$

(b) Poiseullie's equation

$$^{v}/_{t} = \frac{\pi r^4 \Delta P}{8\eta L}; V = \frac{r^2 \Delta P}{8\eta L} \quad (16)$$

$$\Delta P = \frac{8Q\eta L}{\pi r^4} = \frac{8V\eta L}{r^2} \quad (17)$$

2.5.8. Viscosity of nickel suspension.

The viscosity of the suspension was determined using a Brookfield viscometer (LVDVE230, Massachusetts, USA). The suspension was poured on the Buchner funnel containing the nano filters, and the volume of filtrate collected was noted after 5 minutes of recording. The process was repeated thrice to calculate the average volume.

2.6. Heavy metal filtration analysis.

The nickel concentration in the filtrate was analyzed at Springboard Research Laboratory, Awka, using Varian AA240 Atomic Absorption Spectrophotometer, according to APHA 1995 (American Public Health Association). From the observed results, the percentage purity of the filtrate was calculated.

$$\%\ purity = \frac{Conc.\ of\ suspension - conc.\ of\ filtrate}{conc.\ of\ suspension} \times 100 \qquad (18)$$

2.7. Mechanical strength testing.

The mechanical strength of the filter papers was tested using a universal testing machine (Instron, USA) at the Department of Mechanical Engineering, Nnamdi Azikiwe University, Awka, as per ASTM D638 [36]. The tensile strength was measured by applying a load until the filter paper broke. The maximum force applied is the peak force recorded during the test. Then, the strength was evaluated using the formula:

$$Tensile\ strength = \frac{\text{The cross-sectional area of the filter paper}}{\text{Maximum force applied}} \qquad (19)$$

2.8. Statistical analysis.

The statistical analysis involved standard hypothesis testing techniques to evaluate the data. Descriptive statistics, including mean values, standard deviations, and 95% confidence intervals, were computed to provide a summary of the data for each type of filter paper and treatment condition. A one-way analysis of variance (ANOVA) was conducted to compare the means across different groups. The ANOVA assessed whether the group means were statistically different by analyzing the variance between and within the groups. A significant F-value, coupled with a low P-value, indicated that the means of the groups were not equal. The significance level was set at 0.05, which means there was a 5% risk of incorrectly concluding that a difference exists between groups (Type I error). The assumption of equal variances was checked, and a pooled standard deviation was calculated to reflect the overall variability within the groups.

3. Results and Discussion

3.1. Chitosan and nanocellulose particle characteristics for filtration applications.

Table 2 outlines the hydrodynamic diameter, polydispersity index, and zeta potential of chitosan and nanocellulose particles, which are crucial for assessing their effectiveness in filtration applications. The size and stability of these particles are essential for their performance in filtration systems. Both chitosan and nanocellulose particles are nanoscale, but nanocellulose has a significantly smaller hydrodynamic diameter (504.7 nm) than chitosan (891.3 nm). The smaller size of nanocellulose particles enhances their porosity and permeability due to a larger pore size, making them more effective as filtration media [37].

Table 2. Particle size and polydispersity of the particles.

Particles	Hydrodynamic diameter (nm±SD)	Polydispersibility	Zeta-potential (mV±SD)
Chitosan	891.3±4.2	0.521	+60±3.4
Nanocellulose	504.7±12.3	0.312	-46±1.8

Nanocellulose also has a lower polydispersity index (0.312) than chitosan (0.521), indicating a more uniform particle size distribution [38]. This uniformity contributes to the stability and consistency of nanocellulose in filtration applications [39]. Zeta potential is commonly measured to assess nanomaterials' surface charge and stability [40]. The zeta potential values indicate that chitosan has a positive charge (+60±3.4 mV), which can lead to

particle agglomeration, whereas nanocellulose has a negative charge (-46±1.8 mV), promoting better dispersion and stability [41]. The smaller, more uniform particle size and better stability of nanocellulose make it a superior choice for high-performance filtration applications compared to chitosan.

3.2. Physical observation of the nano filters.

The pictorial images of the nano filters are shown in Figure 1. Filter A is distinctly uniform brown, which is characteristic of chitosan material. Chitosan is known for its antibacterial properties and is often used in filtration due to its biocompatibility and biodegradability [21]. Filter B is white with a clear fibrous structure, highlighting the network structure of nanocellulose fibers. Nanocellulose is recognized for its high surface area, mechanical strength, and ability to form a network [42,43], making it suitable for high-performance filtration applications [44]. Filter C (nano cellulose-chitosan) is gray, suggesting a mixture of the two materials and possibly a combination of their properties. Integrating nanocellulose with chitosan could enhance the mechanical strength and filtration efficiency due to the synergistic effects of both materials.

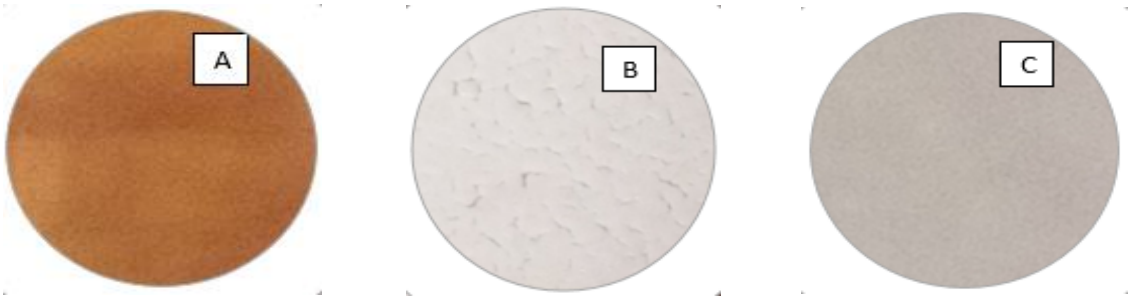

Figure 1. (A) Chitosan filter paper; **(B)** Nanocellulose filter paper; **(C)** Nano cellulose-chitosan filter paper.

3.3. Morphological observation of the nano filters.

The SEM images reveal the morphological characteristics of the nano filters.

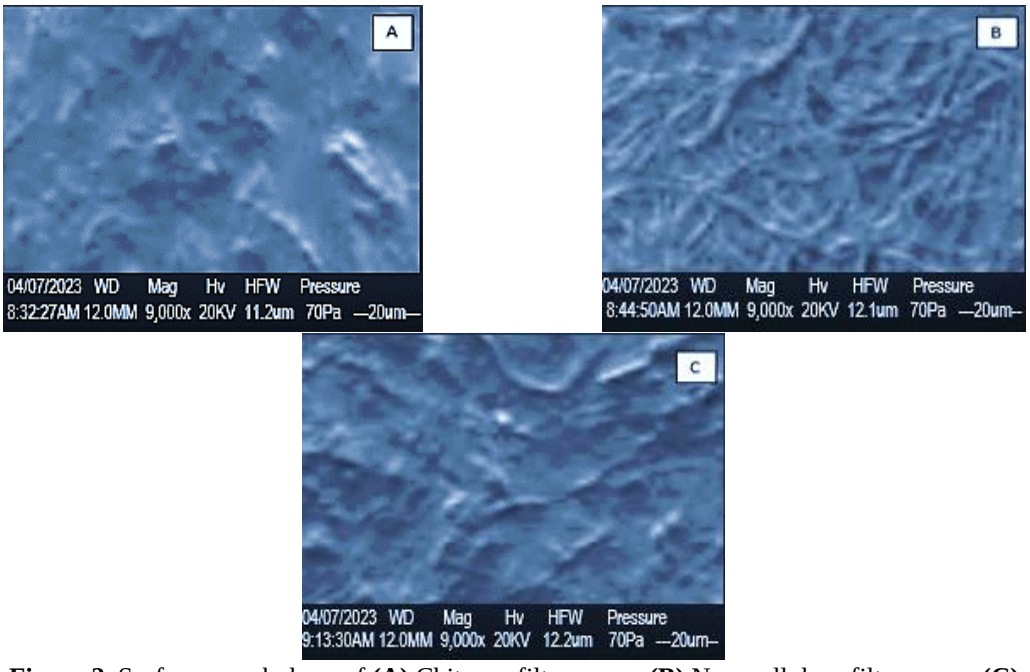

Figure 2. Surface morphology of **(A)** Chitosan filter paper; **(B)** Nanocellulose filter paper; **(C)** Nanocellulose-chitosan filter paper.

The chitosan filter (Figure 2A) shows a smooth surface with uniform pores, indicating well-distributed chitosan particles. The nanocellulose filter (Figure 2B) exhibits a fibrous network with numerous interconnected pores, typical of cellulose fibers, which enhances particle trapping. The nano cellulose-chitosan filter (Figure 2C) displays a homogeneous distribution of nanocellulose and chitosan within the polyacrylamide matrix. The blend of granular and fibrous structures combines the strengths of both materials, leading to improved filtration. The porous structures observed in all images are conducive to high surface area contact with heavy metal ions, enhancing adsorption efficiency.

3.4. Determination of porosity, permeability, and surface area.

Nanocellulose demonstrated higher porosity, permeability, and a larger surface area compared to chitosan, and their combination (Table 3) was determined via equations 3, 5, and 10, respectively. The results show that Batch B, composed of nanocellulose, has the highest porosity at 67%, permeability at 0.1335, and a large surface area. These findings underscore nanocellulose's potential as an advanced material for enhancing filtration efficiency and performance [45]. Nanocellulose's ability to provide substantial porosity facilitates efficient fluid flow. At the same time, its large surface area enhances contact with contaminants, making it particularly advantageous compared to chitosan (Batch A) and the nanocellulose-chitosan combination (Batch C).

Table 3. Porosity, permeability, and surface area of nano filters.

Nano Filters	v1 (m^3)	v2 (m^3)	v3 (m^3)	Viscosity of water (Pa.s)	% Porosity	Permeability (K) m^2	Surface area (S)		Tensile strength (MPa)
							Darcy (m^2/g)	Poiseullie (m^2)	
Batch A	5	5.3±0.05	4.8±0.03	$1.01x10^{-3}$	40	0.0483	0.858	26.67	39.2
Batch B	5	5.5±0.04	4.0±0.06	$1.01x10^{-3}$	67	0.1335	2.034	105.11	82.8
Batch C	5	5.4±0.05	4.3±0.04	$1.01x10^{-3}$	64	0.07683	2.295	89.95	124.6

Nanocellulose exhibited the highest tensile strength due to its fibrous network and high surface area. The nanocellulose filters (Batch B) achieved a tensile strength of 82.8 MPa, indicating a strong material structure. Chitosan had a lower tensile strength of 39.2 MPa due to its less fibrous and more granular structure. Combination filters (Batch C) showed a synergy between chitosan and nanocellulose, resulting in a tensile strength of 124.6 MPa—the combined filter benefits from the strengths of both materials, which will result in improved overall performance. A study by Azeredo et al. [46] also demonstrated that cellulose nanofibers enhance both the mechanical strength and water vapor barrier properties of chitosan films.

3.5. Impact of filtration parameters on nickel suspension at different molarities and pH levels.

The effects of filtration rate, velocity, viscosity, and pressure difference on varied nickel suspension molarities and pH were investigated across different batches of nano filters. The experiments were conducted across multiple batches to capture the nuances in filtration behavior under different chemical conditions. The results show that the filtration characteristics vary significantly depending on the pH and molarity of the nickel suspension (Table 4).

Higher pH levels generally enhance filtration rate and velocity, indicative of improved flow dynamics in alkaline environments. Conversely, acidic conditions reduce these parameters, leading to slower filtration rates and higher pressure differentials across the filter medium. The viscosity of the suspension also plays a critical role, influencing the ease with which particles pass through the filter matrix and affecting overall filtration efficiency.

Furthermore, the purity of the filtrate shows variations across different pH and molarity settings, underscoring the importance of these factors in maintaining product quality during filtration processes.

Table 4. Filtration characteristics of nano filters for nickel suspension.

Nano Filters	0.1 wt% Nickel slurry (100 mg/mL)	Thickness (m)	Area (m^2)	Filtration rate (m^3s^{-1})	Filtration velocity (ms^{-1})	Viscosity of suspension (Pa.s)	Pressure difference Δp (Pa)		Filtrate conc. (mg/mL)	Filtrate purity (%)
							Darcy	Poiseullie		
Batch A	Deionized H_2O (pH 6.8)	$3x10^{-5}$	0.0013	$2\ x10^{-8}$	$1.59x10^{-5}$	$1.98x10^{-3}$ $\pm2.08x10^{-5}$	$1.96x10^{-11}$	$1.89x10^{-8}$	0.000114 $\pm3.21x10^{-6}$	99.9886
	0.1M HCl (pH 1.2)	$3x10^{-5}$	0.0013	$1\ x10^{-8}$	$7.96x10^{-6}$	$2.01x10^{-3}$ $\pm1.34x10^{-5}$	$9.93x10^{-12}$	$9.60x10^{-8}$	0.00103 $\pm3.79x10^{-5}$	99.897
	0.5M HCl (pH 0.4)	$3x10^{-5}$	0.0013	$1\ x10^{-8}$	$7.96x10^{-6}$	$2.13x10^{-3}$ $\pm1.04x10^{-5}$	$1.05x10^{-11}$	$1.02x10^{-8}$	0.00228 $\pm2.89x10^{-5}$	99.772
	0.1M NaOH (pH 13)	$3x10^{-5}$	0.0013	$3\ x10^{-8}$	$2.39x10^{-5}$	$1.99x10^{-3}$ $\pm2.24x10^{-5}$	$2.95x10^{-11}$	$2.85x10^{-8}$	0.000144 $\pm1.01x10^{-6}$	99.9856
	0.5M NaOH (pH 14)	$3x10^{-5}$	0.0013	$5\ x10^{-8}$	$3.98x10^{-5}$	$2.06x10^{-3}$ $\pm1.73x10^{-5}$	$5.09x10^{-11}$	$4.92x10^{-8}$	0.000219 $\pm3.41x10^{-6}$	99.9781
Batch B	Deionized H_2O (pH 6.8)	$3x10^{-5}$	0.0013	$8\ x10^{-8}$	$6.37\ x10^{-5}$	$1.98x10^{-3}$ $\pm2.08x10^{-5}$	$2.83\ x10^{-11}$	$7.56x10^{-8}$	0.000122 $\pm2.65\ x10^{-6}$	99.9878
	0.1M HCl (pH 1.2)	$3x10^{-5}$	0.0013	$1\ x10^{-7}$	$7.96\ x10^{-5}$	$2.01x10^{-3}$ $\pm1.34x10^{-5}$	$3.59\ x10^{-11}$	$9.60x10^{-8}$	0.001278 $\pm3.43x10^{-5}$	99.8722
	0.5M HCl (pH 0.4)	$3x10^{-5}$	0.0013	$1\ x10^{-7}$	$7.96\ x10^{-5}$	$2.13x10^{-3}$ $\pm1.04x10^{-5}$	$3.81\ x10^{-11}$	$1.02x10^{-7}$	0.002814 $\pm1.19\ x10^{-5}$	99.7186
	0.1M NaOH (pH 13)	$3x10^{-5}$	0.0013	$6\ x10^{-8}$	$4.77\ x10^{-5}$	$1.99x10^{-3}$ $\pm2.24x10^{-5}$	$2.14\ x10^{-11}$	$5.70x10^{-8}$	0.000037 $\pm1.53\ x10^{-6}$	99.9963
	0.5M NaOH (pH 14)	$3x10^{-5}$	0.0013	$6\ x10^{-8}$	$4.77\ x10^{-5}$	$2.06\ x10^{-3}$ $\pm1.73x10^{-5}$	$2.21\ x10^{-11}$	$5.90x10^{-8}$	0.000102 $\pm2.51\ x10^{-6}$	99.9898
Batch C	Deionized H_2O (pH 6.8)	$4x10^{-5}$	0.0013	$6\ x10^{-8}$	$4.77\ x10^{-5}$	$1.98x10^{-3}$ $\pm2.08x10^{-5}$	$4.92\ x10^{-11}$	$7.56x10^{-8}$	0.000118 $\pm4.87\ x10^{-6}$	99.9882
	0.1M HCl (pH 1.2)	$4x10^{-5}$	0.0013	$1\ x10^{-7}$	$7.96\ x10^{-5}$	$2.01x10^{-3}$ $\pm1.34x10^{-5}$	$8.33\ x10^{-11}$	$1.28x10^{-7}$	0.001131 $\pm2.15\ x10^{-5}$	99.8869
	0.5M HCl (pH 0.4)	$4x10^{-5}$	0.0013	$1\ x10^{-7}$	$7.96\ x10^{-5}$	$2.13x10^{-3}$ $\pm1.04x10^{-5}$	$8.82\ x10^{-11}$	$1.36x10^{-7}$	0.002781 $\pm4.71\ x10^{-5}$	99.7219
	0.1M NaOH (pH 13)	$4x10^{-5}$	0.0013	$5\ x10^{-8}$	$3.98\ x10^{-5}$	$1.99x10^{-3}$ $\pm2.24x10^{-5}$	$4.12\ x10^{-11}$	$6.33x10^{-8}$	0.000043 $\pm2.13x10^{-6}$	99.9957
	0.5M NaOH (pH 14)	$4x10^{-5}$	0.0013	$4x10^{-8}$	$3.18\ x10^{-5}$	$2.06x10^{-3}$ $\pm1.73x10^{-5}$	$3.41\ x10^{-11}$	$5.25x10^{-8}$	0.000144 $\pm2.44x10^{-6}$	99.9856

Among the three batches of nano filters (A, B, and C), Batch B demonstrates the overall best performance in terms of pressure drop and filtration velocity across different pH conditions. Batch B exhibits relatively lower pressure drops compared to Batches A and C across all pH conditions. In basic conditions (0.1M NaOH and 0.5M NaOH), Batch B also demonstrates lower pressure drops ($2.14\ x10^{-11}$ Pa and $2.21\ x10^{-11}$ Pa, respectively), indicating less resistance in alkaline environments. Batch B exhibits the highest filtration velocities among the three batches across most pH conditions, suggesting faster filtration rates. Even in acidic conditions (0.1M HCl and 0.5M HCl), Batch B maintains high filtration velocities ($7.96\ x10^{-5}$ m/s), demonstrating efficient performance despite increased resistance. While Batch C (nanocellulose-chitosan combination) performed better than Batch A, it did not surpass Batch B regarding pressure drop and filtration velocity. These findings provide valuable insights into the performance of various nano filters under different chemical conditions, guiding the optimization of filtration parameters for nickel suspensions.

3.6. Determination of percentage purity of the nano filters on varied molarities and pH of the nickel suspension.

The performance of polymeric membranes: chitosan filter paper (A), nanocellulose filter paper (B), and nanocellulose-chitosan filter paper (C) are evaluated based on their

separation capabilities [47]. The pH levels of solvents significantly impact the effectiveness of nano filters [48], as evidenced by the varying degrees of nickel purity observed in acidic, neutral, and alkaline environments. Figure 3 demonstrates the percentage purity of nickel removal by nano filters from three different batches (A, B, and C) under varying pH conditions. The data revealed that nano filters maintain high purities, nearing 99.99%, in neutral and basic environments. However, a significant decline in purity is observed in acidic conditions, particularly at lower pH values of 0.4 and 1.2. This decline suggests that acidic environments may compromise the filter materials, reducing filtration efficiency. Batch B, consisting of nanocellulose, tends to perform slightly better in basic conditions than in Batches A and C. Despite this, all batches demonstrate strong filtration performance with minimal variation in purity. These results highlight the role of pH and molarity in selecting nano filters for specific applications, particularly in acidic environments.

The observed decrease in efficiency under acidic conditions could be attributed to the potential degradation or chemical alteration of the nano filter materials when exposed to low pH. This indicates a need for further research into materials that can withstand acidic environments without losing filtration capability. On the other hand, the high efficiency in neutral and basic conditions showcases the robustness and reliability of these filters, making them viable for applications in various industries, including water treatment and chemical processing.

Moreover, the slight superiority of Batch B in basic conditions suggests that nanocellulose may offer some advantages in specific scenarios, possibly due to its unique structural or chemical properties. This insight allows for optimizing nano filter compositions based on the intended operating environment, ensuring maximum efficiency and longevity. The excellent performance of these filters in all pH conditions also suggests their potential for broader industrial and environmental applications, highlighting their versatility and effectiveness.

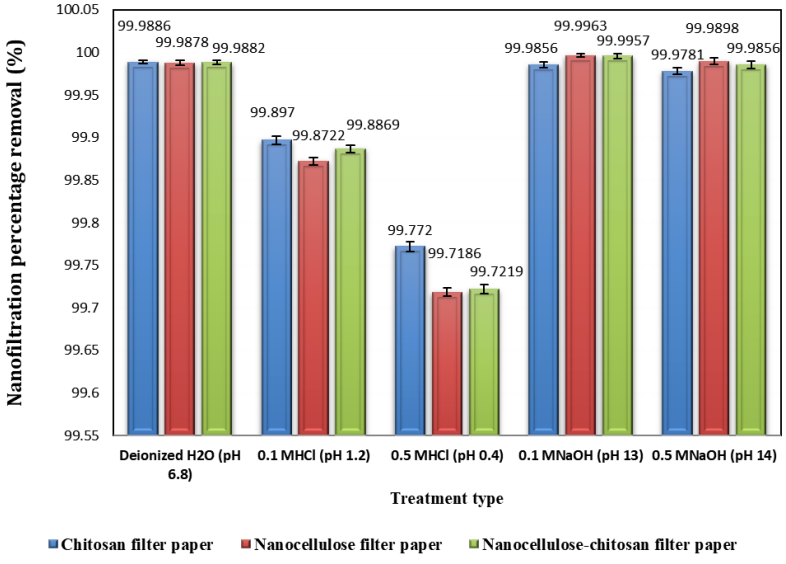

Figure 3. Nanofiltration percentage removals of nickel from water.

3.7. Statistical analysis results.

The objective of the statistical analysis was to examine the performance of three different types of filter papers—chitosan, nanocellulose, and nanocellulose-chitosan—and to assess the effects of different treatment conditions on nanofiltration efficiency. The analysis

began by establishing hypotheses: the null hypothesis proposed that all group means are equal, while the alternative hypothesis suggested that at least one group mean is different. A significance level of 0.05 was applied, and equal variances were assumed throughout the analysis. Descriptive statistics, including mean values and confidence intervals, were calculated for the measured responses to determine if there were any significant differences in the performance of the three filter paper types. ANOVA was then used to test the differences in the means statistically. Additionally, the analysis considered the impact of varying treatment conditions on the nanofiltration performance, focusing on conditions such as deionized H_2O (pH 6.8), 0.1 M HCl (pH 1.2), 0.5 M HCl (pH 0.4), 0.1 M NaOH (pH 13), and 0.5 M NaOH (pH 14).

3.7.1. Performance analysis of three different types of filter paper.

The performance of three different types of filter papers—chitosan, nanocellulose, and nanocellulose-chitosan—was evaluated through descriptive statistics (means and confidence intervals of the measured response) and analysis of variance (ANOVA) to assess whether there are significant differences among them.

The mean values for all three types of filter paper (Table 5) are very similar, indicating no significant difference in their measured responses. The confidence intervals for the means of all three filter paper types overlap considerably, suggesting that any differences in the means are not statistically significant. The pooled standard deviation of 0.110885 is small, reinforcing the conclusion that the variation within each type of filter paper is minimal, and thus, the types of filter paper perform similarly.

Table 5. Mean and standard deviation of the performance of three different types of filter papers.

Factor	N	Mean	StDev	95% CI
Chitosan filter paper	5	99.9243	0.0932	(99.8162, 100.0323)
Nanocellulose filter paper	5	99.9129	0.1203	(99.8049, 100.0210)
Nanocellulose-chitosan filter paper	5	99.9157	0.1172	(99.8076, 100.0237)

Pooled StDev = 0.110885.

The ANOVA results show a P-value of 0.986 (Table 6), which is much higher than the standard significance level of 0.05, indicating that there is no statistically significant difference in the means of the three filter paper types. The low F-value (0.01) further supports the conclusion that the groups have no significant difference. Therefore, the small differences in their means are likely due to random variation rather than any true effect of the filter paper type.

Table 6. One-way ANOVA results for the performance of three different types of filter papers.

Source	DF	Adj SS	Adj MS	F-Value	P-Value
Factor	2	0.000349	0.000175	0.01	0.986
Error	12	0.147545	0.012295		
Total	14	0.147895			

degrees of freedom (DF); sum of squares (Adj SS); mean squares (Adj MS); F-value; P-value.

3.7.2. Impact of treatment conditions on nanofiltration performance.

Statistical analysis of the impact of different treatment conditions on nanofiltration percentage removal reveals key insights. The mean values (Table 7) show that Deionized H_2O and NaOH treatments (both 0.1 M and 0.5 M) result in higher retention rates than HCl

treatments, with 0.5 M HCl showing a significantly lower mean, suggesting a negative impact on performance.

Table 7. Mean and standard deviation of filter paper treatments under different conditions.

Factor	N	Mean	StDev	95% CI
Deionized H_2O (pH 6.8)	3	99.9882	0.0004	(99.9689, 100.0075)
0.1 MHCl (pH 1.2)	3	99.8854	0.0125	(99.8661, 99.9046)
0.5 MHCl (pH 0.4)	3	99.7375	0.0299	(99.7182, 99.7568)
0.1 MNaOH (pH 13)	3	99.9925	0.0060	(99.9733, 100.0118)
0.5 MNaOH (pH 14)	3	99.9845	0.0059	(99.9652, 100.0038)

Pooled StDev = 0.0149824.

The standard deviations are generally low across all treatments (Table 7), but 0.5 M HCl has the highest variability (StDev = 0.0299), indicating less consistent performance under this condition. The 95% confidence intervals for the means overlap for some conditions, particularly between Deionized H_2O and NaOH treatments. However, less overlap is observed with HCl treatments, especially 0.5 M HCl, suggesting a statistically significant difference in performance.

The pooled standard deviation (0.0149824) (Table 7) is small, indicating that while slight differences exist in the means, the overall variability across conditions is low. Given these results, Deionized H_2O, 0.1 M NaOH, and 0.5 M NaOH are identified as the most effective conditions for maintaining high removal efficiency. At the same time, 0.5 M HCl performs the worst among the tested conditions.

The ANOVA results (Table 8) indicate statistically significant differences between the means of the different pH treatments, as evidenced by the very low P-value (<0.05). The high F-value (162.21) suggests that the treatment conditions (different pH levels) have a strong effect on the response variable. Overall, the pH treatments significantly affect the measured response, and the differences between groups are not due to random variation.

Table 8. One-way ANOVA results for filter paper treatments.

Source	DF	Adj SS	Adj MS	F-Value	P-Value
Factor	4	0.145650	0.036412	162.21	0.000
Error	10	0.002245	0.000224		
Total	14	0.147895			

The findings from this study are highly relevant to the use of naturally sourced nanocellulose and chitosan, demonstrating that the methods and insights developed here can be effectively applied to materials derived from agricultural waste. This aligns with the broader goal of creating sustainable, eco-friendly wastewater treatment solutions. The semi-synthetic approach utilized in this research serves as a controlled model, providing a valuable framework for future studies on naturally sourced materials. This ensures that conclusions are robust and applicable across a diverse range of biopolymer sources.

Our research shows that the nanocellulose-chitosan composite not only retains the high adsorption efficiency of its individual components but also surpasses them in performance due to the synergistic interaction between the nanocellulose matrix and the active sites of chitosan. This enhanced performance has not been previously documented in studies focusing solely on nanocellulose or chitosan. Unlike prior research, which predominantly utilized naturally sourced or chemically modified nanocellulose [49,50], this study employs a semi-synthetic preparation method that results in a composite with improved mechanical stability and reusability—attributes critical for practical wastewater treatment applications.

The novelty of this work lies in the innovative combination of nanocellulose and chitosan into a composite membrane, which not only enhances metal ion adsorption efficiency but also provides valuable insights into the scalability of such membranes for treating industrial effluents. Additionally, exploring various surface treatment conditions represents another novel aspect of this study, further contributing to the advancement of filtration technology for environmental applications.

4. Conclusions

This study highlights the superior performance of nanocellulose-based filters over chitosan and composite nanofilters regarding filtration efficiency and mechanical properties. Nanocellulose filters demonstrated the smallest particle size, the highest zeta potential, and a highly interconnected fibrous structure, contributing to their exceptional filtration capabilities. They consistently outperformed chitosan and composite filters in filtration rate, velocity, and filtrate purity across various pH conditions. Specifically, nanocellulose filters achieved the highest filtration velocity of 7.96 x 10^{-5} m/s and filtrate purity of 99.99% with the lowest pressure drop of 2.14x10^{-11} and 2.21 x10^{-11} Pa at basic conditions (0.1M NaOH and 0.5M NaOH, respectively), emphasizing their robustness under alkaline conditions.

Although the ANOVA results indicated no significant difference in the performance between the filter types (P-value = 0.986), suggesting that chitosan, nanocellulose, and nanocellulose-chitosan filters may be used interchangeably depending on the application, the study revealed a strong influence of pH on filtration performance. Specifically, there was a notable decrease in performance under acidic conditions (P-value < 0.05), underscoring the importance of selecting appropriate filters based on specific environmental conditions, especially in applications where pH levels may vary.

These findings highlight nanocellulose's potential as an advanced filtration material, offering enhanced performance for both industrial and environmental applications. This study also contributed to the existing body of knowledge by offering a novel composite material that effectively combines the strengths of both nanocellulose and chitosan, resulting in a highly efficient and sustainable solution for nickel removal from water. This work sets the stage for future research into composite materials that integrate multiple biopolymers, providing a new direction for developing advanced filtration technologies with tailored properties for specific contaminants. Future work will translate these findings to nanocellulose and chitosan directly sourced from agricultural waste. This will help validate the scalability and sustainability of using bio-based materials in real-world wastewater treatment applications. The current study lays the groundwork for such efforts, providing a detailed understanding of the interactions and effectiveness of these materials, whether semi-synthetic or naturally sourced.

Funding

The authors solemnly declare that no external funding was received for this research.

Acknowledgments

We wish to acknowledge Nnamdi Azikiwe Univerity, Nigeria, and Wroclaw University of Environmental and Life Sciences, Poland. The authors wish to acknowledge their father, Prof. Pius Chukwukelue Onyechi.

Conflicts of Interest

The authors declare that there are no conflicts of interest.

References

1. Nishu; Kumar, S. Smart and innovative nanotechnology applications for water purification. *Hybrid Advances* **2023**, *3*, 100044, https://doi.org/10.1016/j.hybadv.2023.100044.
2. Aoudi, B.; Boluk, Y.; Gamal El-Din, M. Recent advances and future perspective on nanocellulose-based materials in diverse water treatment applications. *Science of The Total Environment* **2022**, *843*, 156903, https://doi.org/10.1016/j.scitotenv.2022.156903.
3. Awang, N.A.; Salleh, W.N.W.; Yusof, N.; Karim, Z.A.; Ismail, A.F. Nanocellulose-Based Materials for Heavy Metal Removal from Wastewater. In Environmental Nanotechnology, Dasgupta, N., Ranjan, S., Lichtfouse, E., Mishra, B.N., Eds.; Springer International Publishing: Cham, **2021**; Volume 5, pp. 1-34, https://doi.org/10.1007/978-3-030-73010-9_1.
4. Aniagor, C.O.; Igwegbe, C.A.; Iwuozor, K.O.; Iwuchukwu, F.U.; Eshiemogie, S.; Menkiti, M.C.; Ighalo, J.O. CuO nanoparticles as modifiers for membranes: a review of performance for water treatment. *Materials Today Communications* **2022**, *32*, 103896, https://doi.org/10.1016/j.mtcomm.2022.103896.
5. Mitra, S.; Chakraborty, A.J.; Tareq, A.M.; Emran, T.B.; Nainu, F.; Khusro, A.; Idris, A.M.; Khandaker, M.U.; Osman, H.; Alhumaydhi, F.A.; et al. Impact of heavy metals on the environment and human health: Novel therapeutic insights to counter the toxicity. *Journal of King Saud University - Science* **2022**, *34*, 101865, https://doi.org/10.1016/j.jksus.2022.101865.
6. Sodhi, K.K.; Mishra, L.C.; Singh, C.K.; Kumar, M. Perspective on the heavy metal pollution and recent remediation strategies. *Current Research in Microbial Sciences* **2022**, *3*, 100166, https://doi.org/10.1016/j.crmicr.2022.100166.
7. Igwegbe, C.A.; Onyechi, C.C.; Białowiec, A.; Onukwuli, O.D. Enhancing municipal solid waste leachate treatment efficiency: AI-based prediction of electrocoagulation/flocculation recovery using iron electrodes. *Environmental Technology* **2024**, *45*, 6184-6199, https://doi.org/10.1080/09593330.2024.2328659.
8. Zinicovscaia, I. Conventional Methods of Wastewater Treatment. In Cyanobacteria for Bioremediation of Wastewaters, Zinicovscaia, I., Cepoi, L., Eds.; Springer International Publishing: Cham, **2016**; pp. 17-25, https://doi.org/10.1007/978-3-319-26751-7_3.
9. Egbosiuba, T.C.; Ani, I.J.; Okafor, B.O.; Mustapha, S.; Tijani, J.O.; Igwegbe, C.A.; Okoye, C.C.; Ulakpa, W.C.; Ezennajiego, E.E.; Abdulkareem, A.S. Chapter 6 - Carbon nanotubes–based nanoadsorbents in wastewater treatment. In Adsorption through Advanced Nanoscale Materials, Verma, C., Aslam, J., Khan, M.E., Eds.; Elsevier: **2023**; pp. 103-141, https://doi.org/10.1016/B978-0-443-18456-7.00006-7.
10. Aljlil, S. A Mathematical Simulation of Copper and Nickel Ions Separation Using Prepared Nanocellulose Material. *Membranes* **2023**, *13*, 381, https://doi.org/10.3390/membranes13040381.
11. de Borja Ojembarrena, F.; van Hullebusch, E.; Marsac, R.; Merayo, N.; Blanco, A.; Negro, C. Selective recovery of Co (II), Mn (II), Cu (II), and Ni (II) by multiple step batch treatments with nanocellulose products. *Environmental Science and Pollution Research* **2024**, *31*, 66725–66741, https://doi.org/10.1007/s11356-024-35699-0.
12. Jiang, H.; Wu, S.; Zhou, J. Preparation and modification of nanocellulose and its application to heavy metal adsorption: A review. *International Journal of Biological Macromolecules* **2023**, *236*, 123916, https://doi.org/10.1016/j.ijbiomac.2023.123916.
13. Das, K.K.; Reddy, R.C.; Bagoji, I.B.; Das, S.; Bagali, S.; Mullur, L.; Khodnapur, J.P.; Biradar, M. Primary concept of nickel toxicity–an overview. *Journal of Basic and Clinical Physiology and Pharmacology* **2019**, *30*, 141-152, https://doi.org/10.1515/jbcpp-2017-0171.
14. Genchi, G.; Carocci, A.; Lauria, G.; Sinicropi, M.S.; Catalano, A. Nickel: Human health and environmental toxicology. *International Journal of Environmental Research and Public Health* **2020**, *17*, 679, https://doi.org/10.3390/ijerph17030679.
15. Pradhan, D.; Jaiswal, A.K.; Jaiswal, S. Emerging technologies for the production of nanocellulose from lignocellulosic biomass. *Carbohydrate Polymers* **2022**, *285*, 119258, https://doi.org/10.1016/j.carbpol.2022.119258.

16. Trache, D.; Tarchoun, A.F.; Derradji, M.; Hamidon, T.S.; Masruchin, N.; Brosse, N.; Hussin, M.H. Nanocellulose: from fundamentals to advanced applications. *Frontiers in chemistry* **2020**, *8*, 392, https://doi.org/10.3389/fchem.2020.00392.
17. Norizan, M.N.; Shazleen, S.S.; Alias, A.H.; Sabaruddin, F.A.; Asyraf, M.R.M.; Zainudin, E.S.; Abdullah, N.; Samsudin, M.S.; Kamarudin, S.H.; Norrrahim, M.N.F. Nanocellulose-based nanocomposites for sustainable applications: A review. *Nanomaterials* **2022**, *12*, 3483, https://doi.org/10.3390/nano12193483.
18. Carpenter, A.W.; de Lannoy, C.-F.; Wiesner, M.R. Cellulose nanomaterials in water treatment technologies. *Environmental science & technology* **2015**, *49*, 5277-5287, https://doi.org/10.1021/es506351r.
19. Ai, Y.; Lin, Z.; Zhao, W.; Cui, M.; Qi, W.; Huang, R.; Su, R. Nanocellulose-based hydrogels for drug delivery. *Journal of Materials Chemistry B* **2023**, *11*, 7004-7023, https://doi.org/10.1039/D3TB00478C.
20. Lunardi, V.B.; Soetaredjo, F.E.; Putro, J.N.; Santoso, S.P.; Yuliana, M.; Sunarso, J.; Ju, Y.-H.; Ismadji, S. Nanocelluloses: Sources, pretreatment, isolations, modification, and its application as the drug carriers. *Polymers* **2021**, *13*, 2052, https://doi.org/10.3390/polym13132052.
21. Egorov, A.R.; Kirichuk, A.A.; Rubanik, V.V.; Rubanik Jr, V.V.; Tskhovrebov, A.G.; Kritchenkov, A.S. Chitosan and its derivatives: preparation and antibacterial properties. *Materials* **2023**, *16*, 6076, https://doi.org/10.3390/ma16186076.
22. Ul-Islam, M.; Alabbosh, K.F.; Manan, S.; Khan, S.; Ahmad, F.; Ullah, M.W. Chitosan-based nanostructured biomaterials: Synthesis, properties, and biomedical applications. *Advanced Industrial and Engineering Polymer Research* **2024**, *7*, 79-99, https://doi.org/10.1016/j.aiepr.2023.07.002.
23. Verma, C.; Quraishi, M. Chelation capability of chitosan and chitosan derivatives: Recent developments in sustainable corrosion inhibition and metal decontamination applications. *Current Research in Green and Sustainable Chemistry* **2021**, *4*, 100184, https://doi.org/10.1016/j.crgsc.2021.100184.
24. Guibal, E. Interactions of metal ions with chitosan-based sorbents: a review. *Separation and purification technology* **2004**, *38*, 43-74, https://doi.org/10.1016/j.seppur.2003.10.004.
25. Hamimed, S.; Jebli, N.; Othmani, A.; Hamimed, R.; Barhoum, A.; Chatti, A. Nanocelluloses for Removal of Heavy Metals From Wastewater. In Handbook of Nanocelluloses: Classification, Properties, Fabrication, and Emerging Applications, Barhoum, A., Ed.; Springer International Publishing: Cham, **2022**; pp. 1-42, https://doi.org/10.1007/978-3-030-62976-2_51-1.
26. Heris, S.Z.; Ebadiyan, H.; Mousavi, S.B.; Nami, S.H.; Mohammadpourfard, M. The influence of nano filter elements on pressure drop and pollutant elimination efficiency in town border stations. *Scientific Reports* **2023**, *13*, 18793, https://doi.org/10.1038/s41598-023-46129-5.
27. Buhome, O.; Wongwattanakul, M.; Daduang, J.; Limpaiboon, T. 3D silk fibroin-gelatin/hyaluronic acid/heparan sulfate scaffold enhances expression of stemness and EMT markers in cholangiocarcinoma. *in vivo* **2022**, *36*, 1155-1167, https://doi.org/10.21873/invivo.12815.
28. Alazab, M.H.; Abouelgeit, S.A.; Aboushelib, M.N. Histomorphometric evaluation of 3D printed graphene oxide-enriched poly (ε-caprolactone) scaffolds for bone regeneration. *Heliyon* **2023**, *9*, e15844, https://doi.org/10.1016/j.heliyon.2023.e15844.
29. da Silva, F.M.O.; da Silva, L.G.M.; Justi, A.C.; Rodrigues, M.V.; Aguiar, M.L. Use of hybrid filters to optimize the process of the filtration in cement particles. *Heliyon* **2023**, *9*, e21808, https://doi.org/10.1016/j.heliyon.2023.e21808.
30. Pal, L.; Joyce, M.K.; Fleming, P.D. A simple method for calculation of the permeability coefficient of porous media. *Tappi journal* **2006**, *5*, 10-16.
31. Valdes-Parada, F.J.; Ochoa-Tapia, J.A.; Alvarez-Ramirez, J. Validity of the permeability Carman–Kozeny equation: A volume averaging approach. *Physica A: Statistical Mechanics and its Applications* **2009**, *388*, 789-798, https://doi.org/10.1016/j.physa.2008.11.024.
32. Tiab, D.; Donaldson, E.C. Chapter 3 - Porosity and Permeability. In Petrophysics (Fourth Edition), Tiab, D., Donaldson, E.C., Eds.; Gulf Professional Publishing: Boston, **2016**; pp. 67-186, https://doi.org/10.1016/B978-0-12-803188-9.00003-6.
33. Miyoshi, H.; Nakamura, R.; Noda, Y.; Kimura, H.; Kamiya, S.; Morio, A.; Watanabe, T.; Narasaki, S.; Toyota, Y.; Saeki, N. Relationship Between the Loaded Pressure and Flow Rate of Packed Red Blood Cells and Various Infusion Solutions in Normal Infusion Lines and Catheters. *Anesthesia & Analgesia* **2021**, *133*, 1107-1115, https://doi.org/10.1213/ane.0000000000005700.
34. Bachrun, R.; Pallu, M.; Thaha, M.; Bakri, B. The effect of discharge on head loss with straight and bend flow directions in the pipeline. *IOP Conf. Ser.: Earth Environ. Sci.* **2021**, *841*, 012017, http://dx.doi.org/10.1088/1755-1315/841/1/012017.

35. Liu, G.; Xiao, M.; Zhang, X.; Gal, C.; Chen, X.; Liu, L.; Pan, S.; Wu, J.; Tang, L.; Clements-Croome, D. A review of air filtration technologies for sustainable and healthy building ventilation. *Sustainable Cities and SocietySociety* **2017**, *32*, 375-396, https://doi.org/10.1016/j.scs.2017.04.011.
36. ASTM D638-14. Standard Test Method for Tensile Properties of Plastics. **1998**; https://doi.org/10.1520/D0638-14.
37. Mautner, A.; Bismarck, A. Bacterial nanocellulose papers with high porosity for optimized permeance and rejection of nm-sized pollutants. *Carbohydrate Polymers* **2021**, *251*, 117130, https://doi.org/10.1016/j.carbpol.2020.117130.
38. Danaei, M.; Dehghankhold, M.; Ataei, S.; Hasanzadeh Davarani, F.; Javanmard, R.; Dokhani, A.; Khorasani, S.; Mozafari, M. Impact of particle size and polydispersity index on the clinical applications of lipidic nanocarrier systems. *Pharmaceutics* **2018**, *10*, 57, https://doi.org/10.3390/pharmaceutics10020057.
39. Norrrahim, M.N.F.; Kasim, N.A.M.; Knight, V.F.; Ujang, F.A.; Janudin, N.; Razak, M.A.I.A.; Shah, N.A.A.; Noor, S.A.M.; Jamal, S.H.; Ong, K.K. Nanocellulose: the next super versatile material for the military. *Materials Advances* **2021**, *2*, 1485-1506, https://doi.org/10.1039/D0MA01011A.
40. Sizochenko, N.; Mikolajczyk, A.; Syzochenko, M.; Puzyn, T.; Leszczynski, J. Zeta potentials (ζ) of metal oxide nanoparticles: A meta-analysis of experimental data and a predictive neural networks modeling. *NanoImpact* **2021**, *22*, 100317, https://doi.org/10.1016/j.impact.2021.100317.
41. Németh, Z.; Csóka, I.; Semnani Jazani, R.; Sipos, B.; Haspel, H.; Kozma, G.; Kónya, Z.; Dobó, D.G. Quality by design-driven zeta potential optimisation study of liposomes with charge imparting membrane additives. *Pharmaceutics* **2022**, *14*, 1798, https://doi.org/10.3390/pharmaceutics14091798.
42. Patil, T.V.; Patel, D.K.; Dutta, S.D.; Ganguly, K.; Santra, T.S.; Lim, K.-T. Nanocellulose, a versatile platform: From the delivery of active molecules to tissue engineering applications. *Bioactive materials* **2022**, *9*, 566-589, https://doi.org/10.1016/j.bioactmat.2021.07.006.
43. Carvalho, A.P.A.d.; Értola, R.; Conte-Junior, C.A. Nanocellulose-based platforms as a multipurpose carrier for drug and bioactive compounds: From active packaging to transdermal and anticancer applications. *International Journal of Pharmaceutics* **2024**, *652*, 123851, https://doi.org/10.1016/j.ijpharm.2024.123851.
44. Xiong, Z.; Lin, J.; Li, X.; Bian, F.; Wang, J. Hierarchically structured nanocellulose-implanted air filters for high-efficiency particulate matter removal. *ACS Applied Materials & Interfaces* **2021**, *13*, 12408-12416, https://doi.org/10.1021/acsami.1c01286.
45. Fahma, F.; Febiyanti, I.; Lisdayana, N.; Arnata, I.; Sartika, D. Nanocellulose as a new sustainable material for various applications: A review. *Archives of Materials Science and Engineering* **2021**, *109*, 49-64, http://dx.doi.org/10.5604/01.3001.0015.2624.
46. Azeredo, H.M.; Mattoso, L.H.C.; Avena-Bustillos, R.J.; Filho, G.C.; Munford, M.L.; Wood, D.; McHugh, T.H. Nanocellulose reinforced chitosan composite films as affected by nanofiller loading and plasticizer content. *Journal of Food Science* **2010**, *75*, N1-N7, https://doi.org/10.1111/j.1750-3841.2009.01386.x.
47. Khdary, N.H.; Almuarqab, B.T.; El Enany, G. Nanoparticle-embedded polymers and their applications: a review. *Membranes* **2023**, *13*, 537, https://doi.org/10.3390/membranes13050537.
48. Luo, J.; Wan, Y. Effects of pH and salt on nanofiltration—a critical review. *Journal of Membrane Science* **2013**, *438*, 18-28, https://doi.org/10.1016/j.memsci.2013.03.029.
49. Goswami, R.; Mishra, A.; Bhatt, N.; Mishra, A.; Naithani, P. Potential of chitosan/nanocellulose based composite membrane for the removal of heavy metal (chromium ion). *Materials Today: Proceedings* **2021**, *46*, 10954-10959, https://doi.org/10.1016/j.matpr.2021.02.036.
50. Peter, S.; Lyczko, N.; Thomas, S.; Leruth, D.; Germeau, A.; Fati, D.; Nzihou, A. Fabrication of eco-friendly nanocellulose-chitosan-calcium Phosphate ternary nanocomposite for wastewater remediation. *Chemosphere* **2024**, *363*, 142779, https://doi.org/10.1016/j.chemosphere.2024.142779.

Supplementary materials

Table S1. Data for plotting graph of log v/t against log 1/L to determine permeability (k) through the Darcy's equation.

Nano Filters	Filter medium configurations	Filtration/ flow rate Q = v/t (M^3s^{-1})	Thickness L (M)	1/L	Log (Q =v/t)	Log (1/L)	Log X	X
Batch A	L1	0.1033±0.14	3E-05	3E05	-0.9859	5.4771	-1.2212	0.0601
	L2	0.0688±1.36	6E-05	6E05	-1.1624	5.7782		
	L3	0.0355±0.76	9E-05	9E05	-1.4498	5.9542		
	L4	0.0178±2.34	1.2E-06	1.2E06	-1.7495	6.0792		
Batch B	L1	0.1912±1.56	3E-05	3E05	-0.7185	5.4771	-0.7796	0.0166
	L2	0.15±1.62	6E-05	6E05	-0.8239	5.7782		
	L3	0.1011±0.34	9E-05	9E05	-0.9952	5.9542		
	L4	0.061±2.5	1.2E-06	1.2E06	-1.2147	6.0792		
Batch C	L1	0.1645±0.43	4E-05	4E05	-0.7838	5.6021	-1.0194	0.0957
	L2	0.1221±1.55	8E-05	8E05	-0.9133	5.9031		
	L3	0.0688±1.02	1.2E-06	1.2E06	-1.1624	6.0792		
	L4	0.0378±2.41	1.6E-06	1.6E06	-1.4225	6.2041		

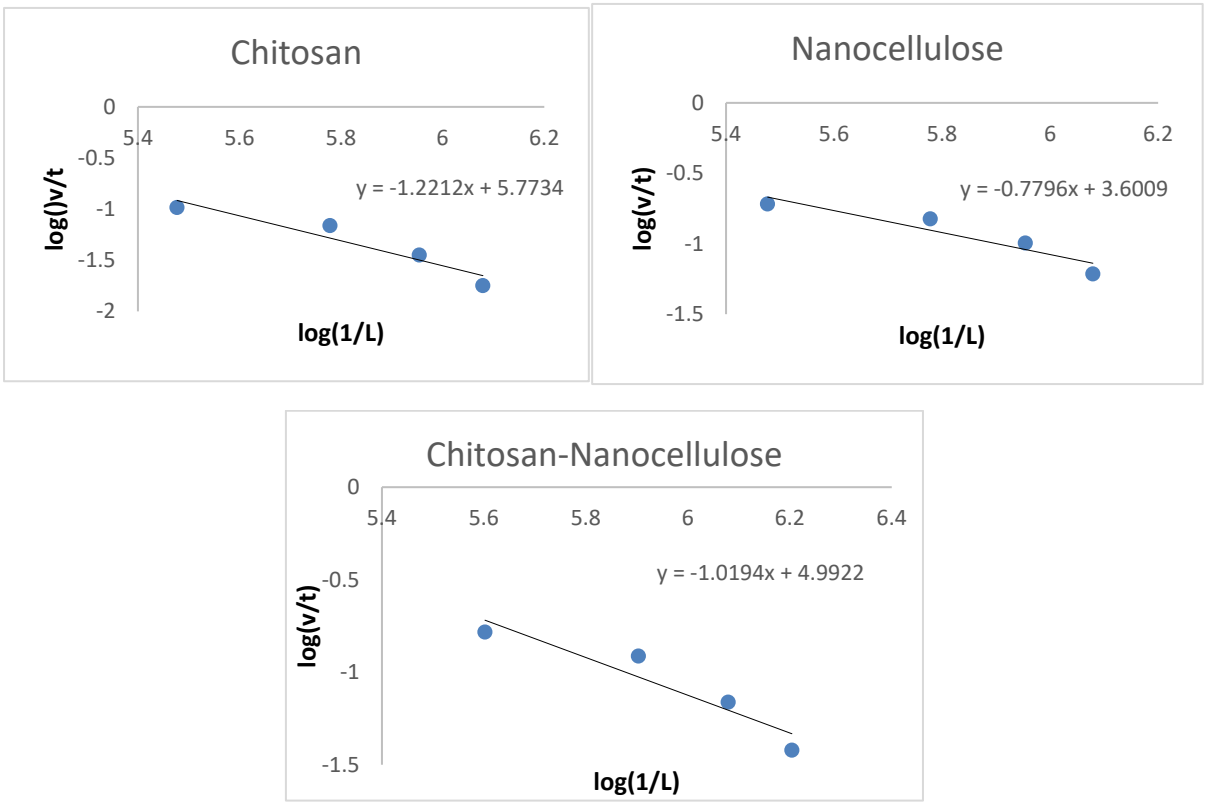

Figure S1. A graph of log v/t against log 1/L was plotted to determine permeability (k) through the Darcy's equation.

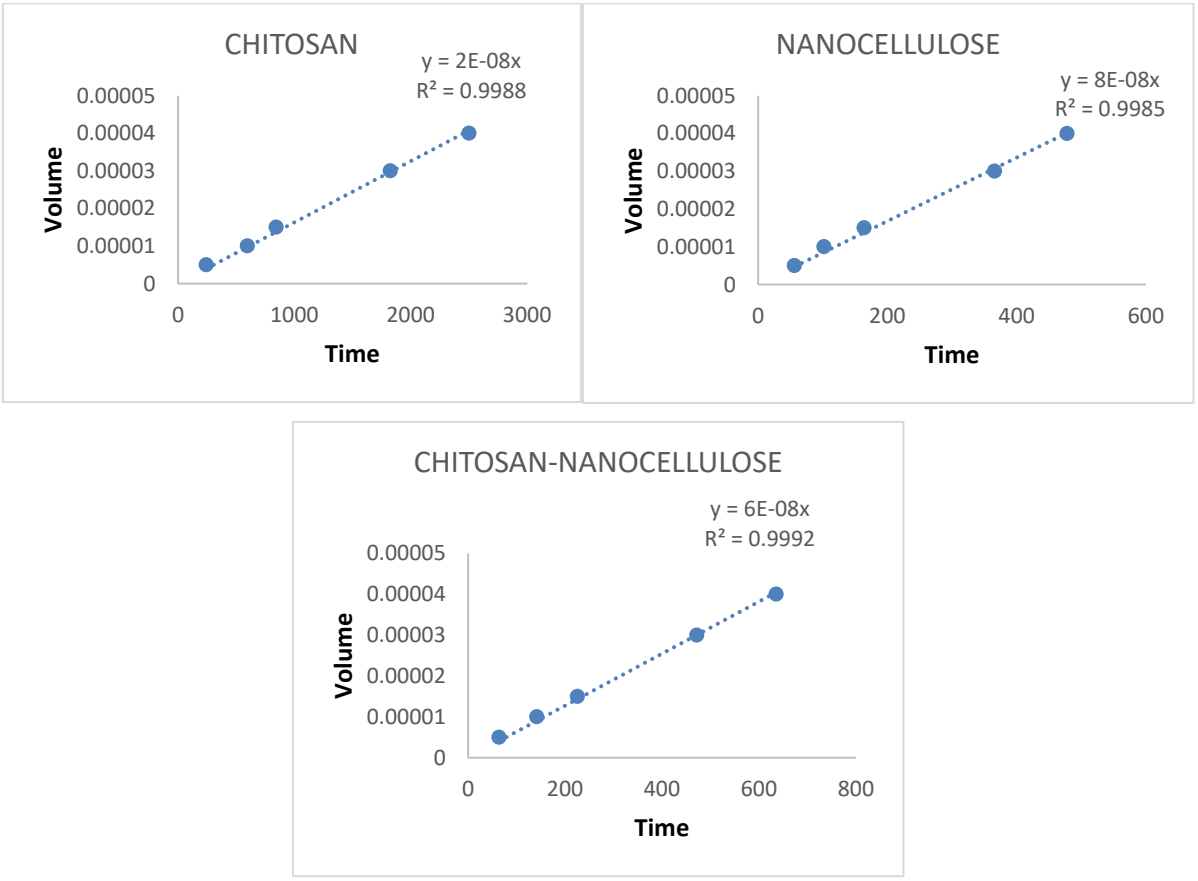

Figure S2a. A graph of volume of filtrate against time for deionized water (pH).

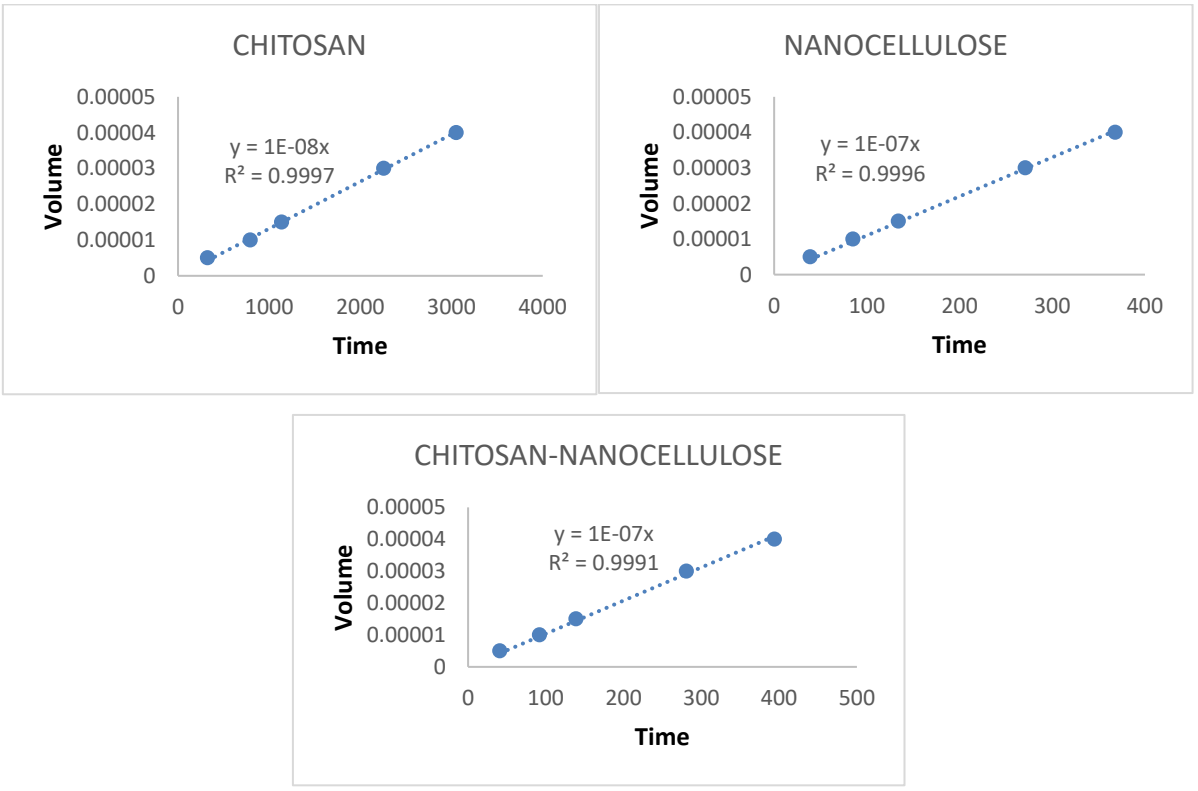

Figure S2b. A graph of volume of filtrate against time for 0.1 M HCl (pH 1.2).

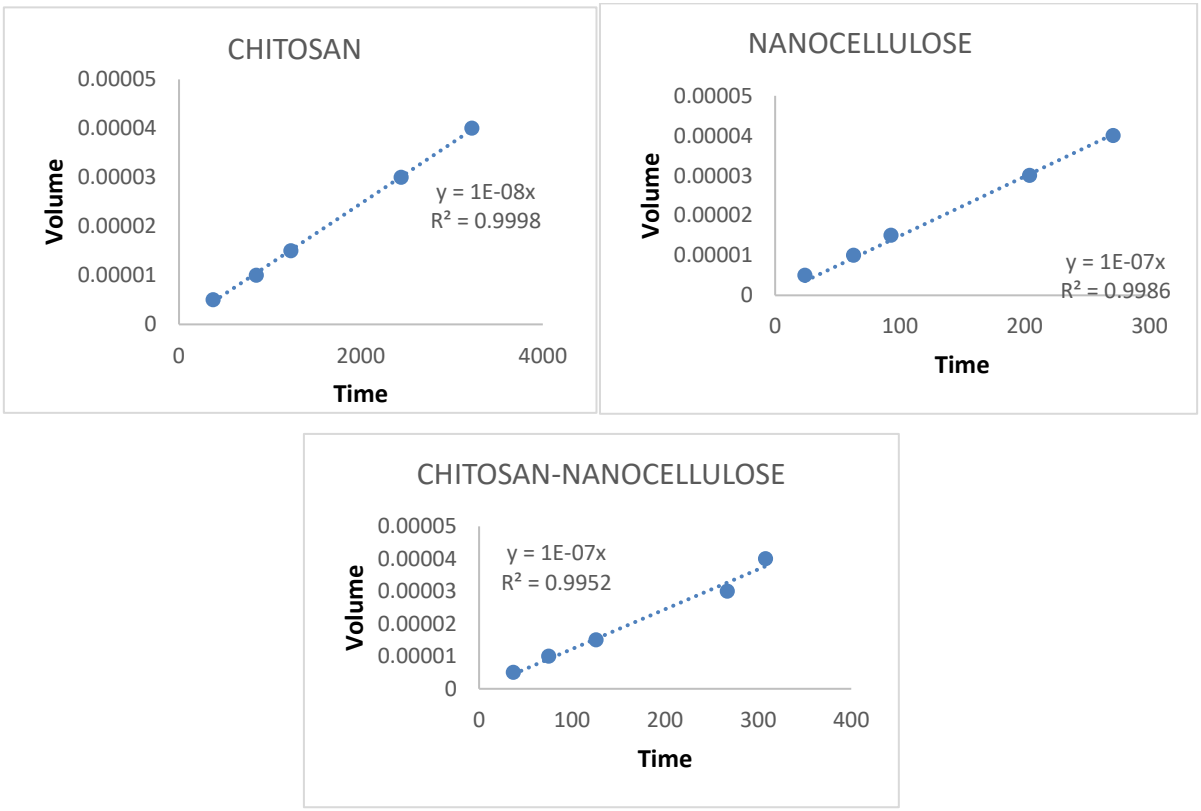

Figure S2c. A graph of volume of filtrate against time for 0.5 M HCl (pH 0.4).

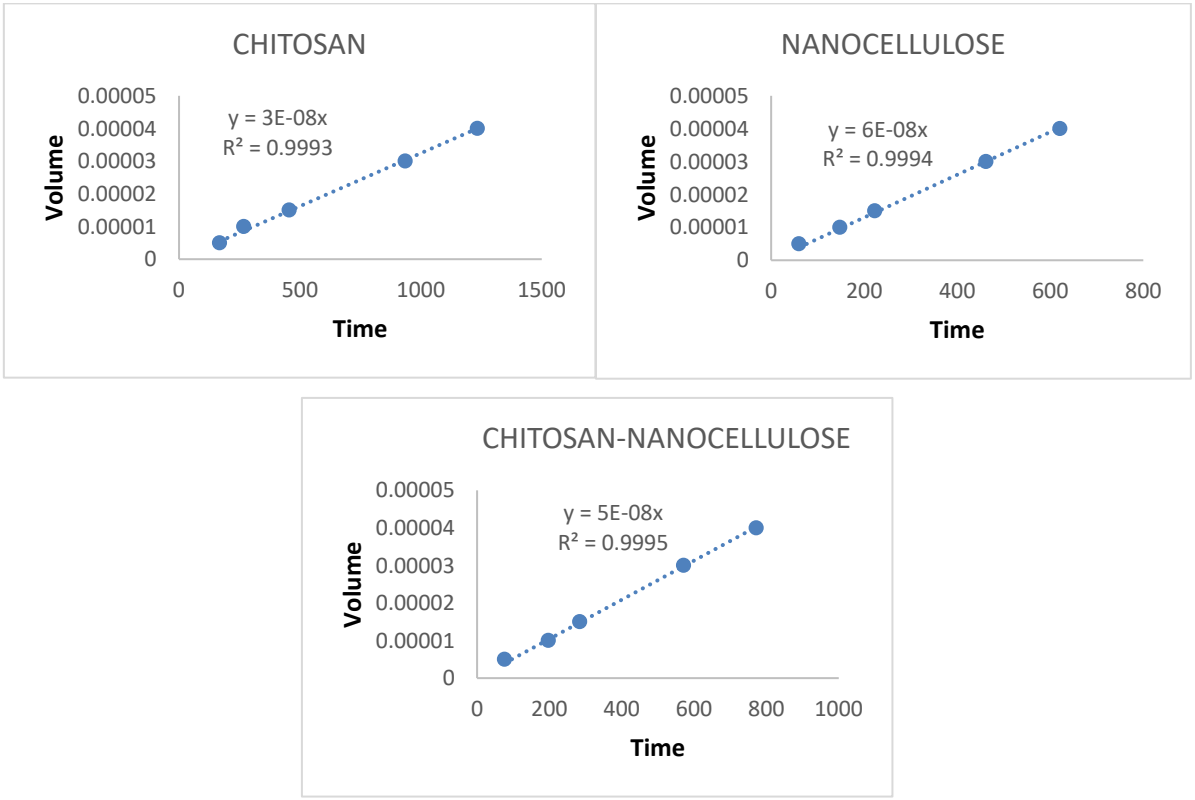

Figure S2d. A graph of volume of filtrate against time for 0.1 M NaOH (pH 13).

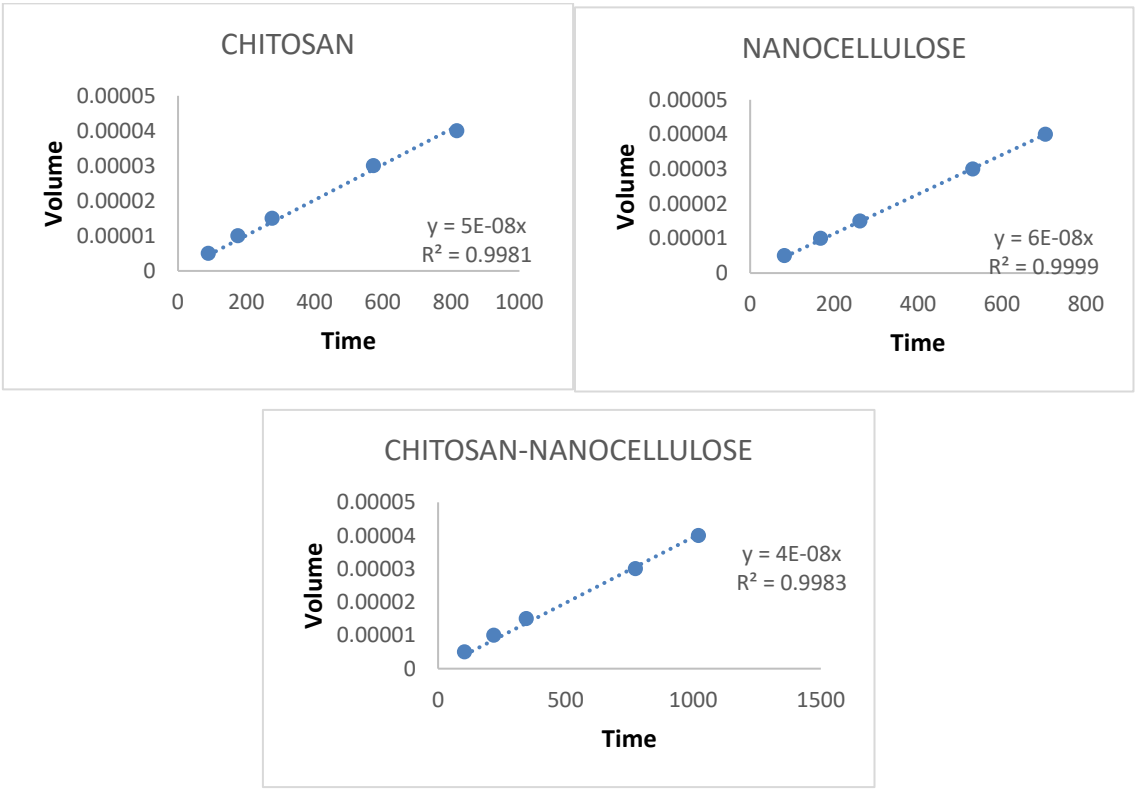

Figure S2e. A graph of volume of filtrate against time for 0.5 M NaOH (pH 14).

Table S2. Data from Figure S1 for Q determinations.

Nano Filter Batch A			
10 wt% Nickel slurry (100 mg/ml)	Filtration volume v (M^3)	Time t (s)	Filtration/ flow rate Q = v/t (M^3s^{-1})
Deionized water (pH 6.8)	0.000005	243±5.11	2.00E-08
	0.00001	596±4.34	
	0.000015	844±8.09	
	0.00003	1824±5.54	
	0.00004	2501±3.21	
0.1M HCl (pH 1.2)	0.000005	324±6.3	1.00E-08
	0.00001	793±10.34	
	0.000015	1137±3.44	
	0.00003	2256±3.33	
	0.00004	3051±7.45	
0.5M HCl (pH 0.4)	0.000005	376±2.56	1.00E-08
	0.00001	852±6.77	
	0.000015	1232±11.04	
	0.00003	2444±5.98	
	0.00004	3221±3.57	
0.1M NaOH (pH 13)	0.000005	168±5.6	3.00E-08
	0.00001	268±2.44	
	0.000015	456±7.47	
	0.00003	936±9.41	
	0.00004	1234±12.13	
0.5M NaOH (pH 14)	0.000005	89±1.99	5.00E-08
	0.00001	176±5.22	
	0.000015	276±8.3	
	0.00003	573±5.67	
	0.00004	817±4.78	
Nano Filter Batch B			
10 wt% Nickel slurry (100 mg/ml)	Filtration volume v (M^3)	Time t (s)	Filtration/ flow rate Q = v/t (M^3s^{-1})
Deionized water (pH 6.8)	0.000005	56±1.57	8.00E-08

	0.00001	102±5.73	
	0.000015	164±9.24	
	0.00003	366±7.82	
	0.00004	478±5.44	
0.1M HCl (pH 1.2)	0.000005	39±2.83	1.00E-07
	0.00001	85±4.61	
	0.000015	134±5.76	
	0.00003	271±9.75	
	0.00004	368±5.42	
0.5M HCl (pH 0.4)	0.000005	24±8.66	1.00E-07
	0.00001	63±6.77	
	0.000015	93±3.22	
	0.00003	204±5.35	
	0.00004	271±6.33	
0.1M NaOH (pH 13)	0.000005	60±1.98	6.00E-08
	0.00001	148±5.01	
	0.000015	223±7.43	
	0.00003	462±6.71	
	0.00004	621±6.82	
0.5M NaOH (pH 14)	0.000005	82±3.43	6.00E-08
	0.00001	168±8.55	
	0.000015	262±11.09	
	0.00003	531±6.99	
	0.00004	704±8.76	
Nano Filter Batch C			
10 wt% Nickel slurry (100 mg/ml)	Filtration volume v (M^3)	Time t (s)	Filtration/ flow rate Q = v/t (M^3s^{-1})
Deionized water (pH 6.8)	0.000005	64±2.54	6.00E-08
	0.00001	142±1.45	
	0.000015	226±7.89	
	0.00003	472±4.32	
	0.00004	636±9.45	
0.1M HCl (pH 1.2)	0.000005	41±2.65	1.00E-07
	0.00001	92±5.89	
	0.000015	139±7.44	
	0.00003	281±10.31	
	0.00004	394±6.29	
0.5M HCl (pH 0.4)	0.000005	37±4.38	1.00E-07
	0.00001	75±6.33	
	0.000015	126±3.77	
	0.00003	267±5.45	
	0.00004	308±9.38	
0.1M NaOH (pH 13)	0.000005	76±4.67	5.00E-08
	0.00001	197±8.11	
	0.000015	284±6.05	
	0.00003	571±3.67	
	0.00004	772±6.12	
0.5M NaOH (pH 14)	0.000005	104±3.81	4.00E-08
	0.00001	219±3.56	
	0.000015	346±6.77	
	0.00003	774±5.98	
	0.00004	1021±6.42	